143 (2022) 213185

Contents lists available at ScienceDirect

Biomaterials Advances

journal homepage: www.journals.elsevier.com/materials-science-and-engineering-c

Bioactivated gellan gum hydrogels affect cellular rearrangement and cell response in vascular co-culture and subcutaneous implant models

Christine Gering [a,*], Jenny Párraga [a,1], Hanna Vuorenpää [a,b], Lucía Botero [c], Susanna Miettinen [a,b], Minna Kellomäki [a]

[a] Faculty of Medicine and Health Technology, Tampere University, Tampere, Finland
[b] Research, Development and Innovation Centre, Tampere University Hospital, Tampere, Finland
[c] Facultad de Medicina Veterinaria y de Zootecnia, Universidad Nacional de Colombia, Bogotá, Colombia

ARTICLE INFO

Keywords:
Vascularization
HUVEC and hASC co-culture
Gellan gum hydrogels
Biofunctionalization
Mechanical and viscoelastic properties

ABSTRACT

Hydrogels are suitable soft tissue mimics and capable of creating pre-vascularized tissues, that are useful for *in vitro* tissue engineering and *in vivo* regenerative medicine. The polysaccharide gellan gum (GG) offers an intriguing matrix material but requires bioactivation in order to support cell attachment and transfer of biomechanical cues. Here, four versatile modifications were investigated: Purified NaGG; avidin-modified NaGG combined with biotinylated fibronectin (NaGG-avd); oxidized GG (GGox) covalently modified with carbohydrazide-modified gelatin (gelaCDH) or adipic hydrazide-modified gelatin (gelaADH). All materials were subjected to rheological analysis to assess their viscoelastic properties, using a time sweep for gelation analysis, and subsequent amplitude sweep of the formed hydrogels. The sweeps show that NaGG and NaGG-avd are rather brittle, while gelatin-based hydrogels are more elastic. The degradation of preformed hydrogels in cell culture medium was analyzed with an amplitude sweep and show that gelatin-containing hydrogels degrade more dramatically. A co-culture of GFP-tagged HUVEC and hASC was performed to induce vascular network formation in 3D for up to 14 days. Immunofluorescence staining of the αSMA^{+} network showed increased cell response to gelatin-GG networks, while the NaGG-based hydrogels did not allow for the elongation of cells. Preformed, 3D hydrogels disks were implanted to subcutaneous rat skin pockets to evaluate biological *in vivo* response. As visible from the hematoxylin and eosin-stained tissue slices, all materials are biocompatible, however gelatin-GG hydrogels produced a stronger host response. This work indicates, that besides the biochemical cues added to the GG hydrogels, also their viscoelasticity greatly influences the biological response.

1. Introduction

Hydrogels have extensively been studied for vascular tissue engineering, due to their innate soft material properties, ability to allow encapsulation and nutrient diffusion. Moreover, hydrogels are designed to guide tissue formation for various applications including artificial tissue mimics and *in vivo* regenerative implants. Vascularization, the formation of a perfusable vessel network in artificial tissues, is among the top challenges that impede the clinical application of engineered transplantable tissues [1]. Likewise, *in vitro* models and organ-on-chip applications require vasculature to adequately model living tissues and organs. To create cell support matrix for those, biomaterial design has to be balanced between high bioactivity and rapid cell resorption [2–4], and adequate mechanical and viscoelastic properties [5].

Mechanical and rheological properties are furthermore a concern for the stability of the cell-laden hydrogel and manipulation for different applications, such as injection and casting [5] and others [6–8]. The effect of hydrogel stiffness and elasticity is finding increasing appreciation in tissue engineering literature, and the phenomenon of mechanotransduction from the extracellular network to the cell is essential to biomaterial design [3,9]. Independent of cell adhesive motifs, it is well known that substrate stiffness can direct stem cell differentiation [10]. Moreover, vascular network models have been found to require surrounding matrices that are compliant enough to allow remodeling by cells, but also strong enough to confer mechanical information to the cells [5].

* Corresponding author at: Faculty of Medicine and Health Technology, Korkeaoulunkatu 3, 33720 Tampere, Finland.
E-mail address: christine.gering@tuni.fi (C. Gering).
[1] Currently at IamFluidics BV, High Tech Factory, Enschede, the Netherlands.

https://doi.org/10.1016/j.bioadv.2022.213185
Received 7 June 2022; Received in revised form 28 October 2022; Accepted 1 November 2022
Available online 8 November 2022

Gellan gum (GG) has been investigated for cell and drug delivery due to its gelation properties and cytocompatibility [11–14]. However, only few studies investigate GG hydrogels for vascularization models. One excellent example is given by Rocha et al. who use RGD-conjugated GG (GG-GRGDS) to develop a material for spinal cord injury (SCI) treatment [15]. This GG modification with the peptide sequence RGD *via* furan modification was first described by Silva et al. (2012) [16]. The SCI trauma site has increased need for oxygenation, which can be addressed only with functional vascular network in the transplant. A large array of other biomaterials has been investigated in the literature for vascularization, where the most prominent examples are fibrin and collagen I. In combination with collagen [17] and gelatin-based matrices [18], Human adipose-derived stem/stromal cells (hASC) have been shown to support the formation of formidable tubular networks when in co-culture with an endothelial cell type [15,17,19–21].

To establish stable vascularization, the stromal cell type is needed to support the vascular network formed by endothelial cells (EC). Here, we demonstrate the vascularization potential of a co-culture between human umbilical vein EC (HUVEC) and hASC. hASC are known to promote vascular growth, maturation and stabilization by secreting angiogenic factors and by differentiating into vessel lining supporting cells [19]. Furthermore, high proliferation and differentiation capacity of hASC makes them an ideal component for tissue engineering [19], and they have shown pericytic function when co-cultured with HUVEC. HUVEC are a robust source of EC with relatively easy access and proven capability for capillary morphogenesis. Despite their venous and macrovascular origin, they are the most widely used EC type in tissue engineering application with biomaterials [22]. Recently, we reported the vasculogenic potency of both bone marrow- and adipose tissue-derived mesenchymal stem/stromal in establishing a stable vascular network in fibrin hydrogel [23].

Herein, four different GG hydrogel formulations and modifications are investigated. These materials have been developed and published by us previously, and we considered these four most valuable for comparison and further study. Purified (NaGG) (Fig. 1A) and avidin-modified purified (NaGG-avd) (Fig. 1B) have previously been investigated by us for a modular design [24]. Similarly, the gelatin-gellan gum compound hydrogels, achieved *via* hydrazone crosslinking of oxidized GG and carbohydrazide (gelaCDH) (Fig. 1C) or adipic acid hydrazide (gelaADH) (Fig. 1D) functionalized gelatin, have been investigated for iPSC-derived cardiomyocyte culture by us [25]. While all four materials are based on the polysaccharide GG there are inherent mechanical differences as well. NaGG and NaGG-avd exhibit almost identical brittle compression behavior, but our gelatin-GG hydrogels exhibit an elastic component in their stress–strain curve, closely resembling heart tissue. Though biocompatible, native GG is highly bioinert [26,27], but bioactive functionalization has been shown to improve cell response while maintaining mechanical stability [24,25,28].

2. Materials and methods

GG (Gelzan™ CM-Gelrite®, low acyl form, 1000 kg/mol, CAS 71010-52-1), crosslinkers spermidine trihydrochloride (SPD, 99 %, CAS 334-50-9) and $CaCl_2$ xH_2O (CAS 22691-02-7) as well as other chemicals we purchased from Sigma (now Merck Sigma). Gelatin was purchased from Rousselot (X-Pure®) and Sigma (Gelatin from porcine skin, Type A, gel strength 300). Cytocompatibility of the different gelatin sources was assessed as shown in Appendix 6. Charge-neutralized chimeric avidin (avd) was synthesized and kindly donated by the Protein Dynamics group at Tampere University [29]. Cell culture supplies used for expansion and culture include αMEM (Gibco™, ref. 22561-021), EGM-2 (endothelial cell growth medium-2 BulletKit™, CC-3156, Lonza Group Ltd., Switzerland), and human serum (HS, Serana Europe GmbH, ref. S-HU-EU-011). Reagents for immunohistochemical staining and other analysis were purchased from Merck.

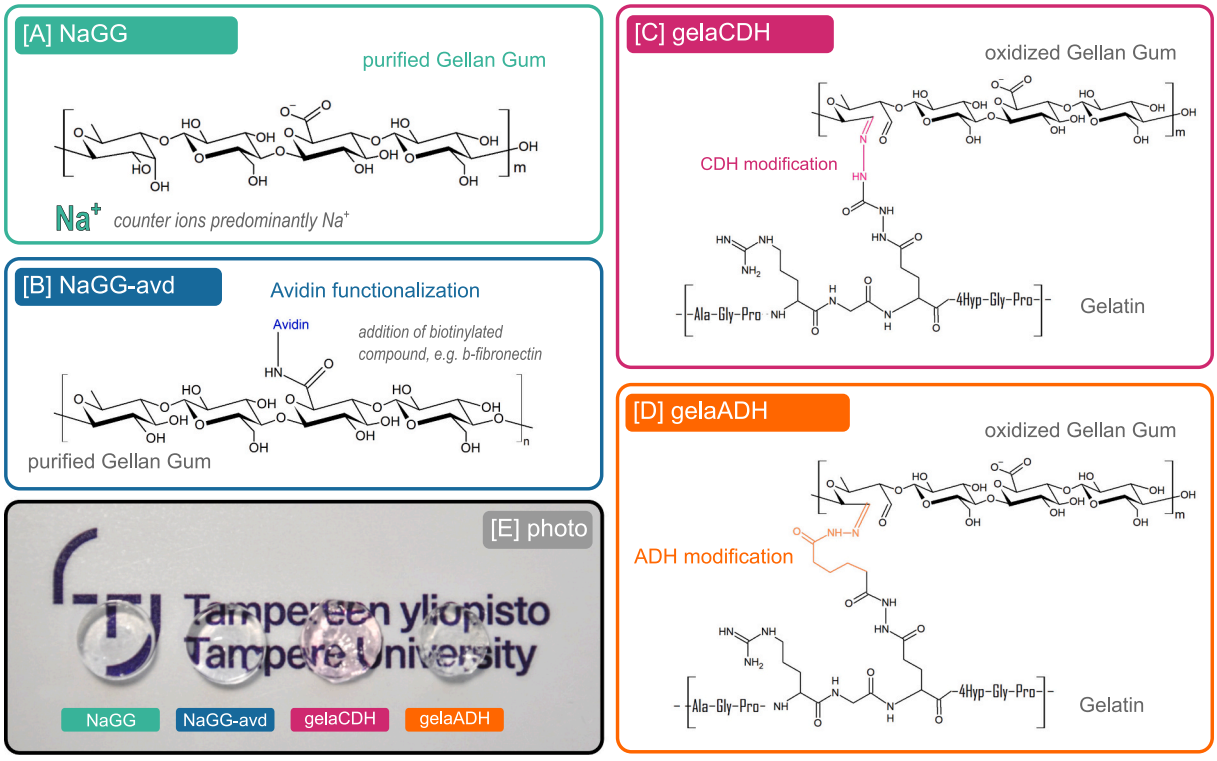

Fig. 1. Chemical structures and exemplary photographs of the investigated materials. [A] Sodium-purified gellan gum (NaGG); [B] purified gellan gum further functionalized with charge-neutralized chimeric avidin (NaGG-avd); [C] Oxidized gellan gum coupled to carbohydrazide-modified gelatin (gelaCDH-GGox); [D] Oxidized gellan gum coupled to adipic acid hydrazide-modified gelatin (gelaADH-GGox). [E] shows a photograph of cell-free hydrogel samples, depicting their ability to self-support and transparency.

2.1. Hydrogel modification and preparation

GG was purified and coupled with avidin according to [24]. Briefly, counterions were removed from commercial GG formulations using exchange resin (Dowex cation exchange resin, H+ form, 50–100 mesh, prerinsed in HCl) and replaced with sodium (Na^+) to a solution pH of 7.5. NaGG was precipitated in isopropanol and lyophilized. GG was oxidized using Malaprade oxidation, for which a hot (40 °C) GG solution is treated with $NaIO_4$ in a ratio of 50 mg GG to 6 mg $NaIO_4$. The reaction was quenched after 4 h using ethylene glycol and dialyzed (12–14 kDa MWCO) against deionized (DI) water for 3 days before lyophilization [24,25,30].

The gelatin modification protocol was adapted from Koivisto et al. (2019) [25]. Briefly, gelatin was dissolved in ultra-pure water at 2.0 g/L and kept in N_2 environment at room temperature. An excess of carbohydrazide (CDH) or adipic hydrazide (ADH) and the pH was adjusted to 4.7 and 5.0 respectively. A mixture of EDC (100 mg) and HOBT (70 mg) was dissolved in DMSO and dropwise but swiftly added to the gelatin solution. The EDC-HOBT addition was repeated 2 times, to achieve a total molar ratio of 3.8 mM EDC to 21.9 mM CDH or 43.4 mM ADH, respectively. The reaction is kept overnight, and the product is precipitated *via* salting-out using cold ethanol. The precipitate is collected, centrifuged and redissolved into ultra-pure water for dialysis over 2 days. Before lyophilization, the solution is sterile filtered using 0.2 μm syringe filter (Whatman FP30/0.2 CA-S). Hydrogel compositions are based on our previous publications [24,25,30].

Hydrogels were prepared by combination of component 1 (gellan gum) and component 2 (crosslinker) with ratios as listed in Table 1. The components were either mixed in a separate vial (Hydrogel 1 and 2) and cast to the mold or mixed directly in the mold (Hydrogel 3 and 4) to achieve homogenous, bubble-free samples. For cell encapsulation, the cell pellet was resuspended in either component 1 (NaGG and NaGG-avd for Hydrogel 1 and 2), or component 2 (gelaCDH and gelaADH) based on volume and ease of pipetting, and the hydrogels were formed as described above. Only for cell culture experiments, biotinylated fibronectin (2.5 mg/mL stock), synthesized and kindly donated by the Protein Dynamics group at Tampere University, was added to NaGG-avd to achieve a final concentration of 31 μg per mL hydrogel. After casting, the hydrogels are left to set at 37 °C for at least 20 min to 4 h before further manipulation. All components were sterile filtered using a 0.2 μm syringe filter (Whatman FP30/0.2 CA-S).

2.2. Mechanical analysis and degradation

For all rheological experiments, Rheometer DHR-2 (TA Instruments) and 20 mm stainless steel flat geometry were used. To flow test the hydrogel precursors, 370 μL of each solution was pipetted onto the bottom plate and tested using a gap of 1000 μm and analyzed from 0.1 to 500 Hz. Gel formation was observed using a time sweep. The first component of the gel, (NaGG, NaGG-avd, gelaCDH, or gelaADH, was placed to the plate at 37 °C and the geometry was lowered to a gap of 1500 μm. The second component ($CaCl_2$, SPD, or GGox) was added while the geometry was spinning at 7 rad/s for 7 s in order to facilitate mixing, after which the temperature is lowered to 30 °C. The time sweep measurement is started immediately after the spinning step, and run with constant amplitude (0.75 % oscillation strain) and frequency (0.75 Hz) for 3600 s. Consequently, the sample formed during the time sweep was left to rest in place for 5 min and then used for an amplitude sweep. The amplitude sweep was performed from 0.1 % to up to 500 % oscillation strain at 0.75 Hz.

Samples for degradation analysis were prepared as described as cell-free hydrogel in either a ø 20 mm mold for rheological testing at a volume of 500 μL (sample height ~ 2 mm), or in ø 8.8 mm mold for mass loss analysis at a volume of 300 μL (sample height ~ 5 mm). After the hydrogels were fully set (4 h at 37 °C), the samples were chilled overnight at +4 °C to facilitate demolding. Mass loss samples were placed on mesh ring holder, while rheology samples were kept in their molds, and the samples were then incubated with cell culture on top. Mass loss samples were periodically weighed, and new medium was placed on top of the same samples. Rheology samples were finally demolded and analyzed using an amplitude sweep (0.01–500 %) with a fixed frequency of 0.75 Hz and plate temperature of 30 °C. Samples were carefully placed on the bottom geometry and the upper one was brought into contact with the sample so that the axial force was about 0.1 N, ensuring good contact between sample and geometry, without loading too high stress onto the material.

Table 1
Composition of investigated hydrogels. Abbreviation of materials used throughout the text are bolded.

	Component 1 (gellan gum)	Component 2 (crosslinker)	Mixing ratio
1	**NaGG** 5 mg/mL in HEPES/sucrose	Calcium chloride ($CaCl_2$ xH_2O) 10 mM in HEPES/sucrose	5:1
2	**NaGG-avd** 5 mg/mL in HEPES/sucrose	Spermidine trihydrochloride (SPD) 2 mM in HEPES/sucrose	5:1
3	GGox(60) 40 mg/mL in EBM-2	**gelaCDH** 40 mg/mL in EBM-2	1:1
4	GGox(60) 40 mg/mL in sucrose	**gelaADH** 40 mg/mL in sucrose	1:1

2.3. Cell isolation and culture

Human adipose stem/stromal cells (hASC) were isolated from subcutaneous tissue samples obtained from three independent donors to reveal the possible biological variabilities between human donors. Tissue samples were obtained at the Tampere University Hospital Department of Plastic Surgery with the donor's written informed consent and processed under ethical approval of the Ethics Committee of the Expert Responsibility area of Tampere University Hospital (R15161). The cells were isolated as described previously [31]. The hASC were cultured in α-MEM (Thermo Scientific #22561054) supplemented with 5 % HS (HS, Serana Europe GmbH, ref. S-HU-EU-011), 100 U/mL penicillin, and 100 μg/mL streptomycin, expanded over 4 days and used between passages 1–3. The mesenchymal origin of hASC was confirmed by surface marker expression analysis with flow cytometry and assessment of adipogenic and osteogenic differentiation potential according to the International Society for Cellular Therapy criteria [32].

Human umbilical vein endothelial cells (HUVEC) pooled from several human donors were expressing green fluorescent protein (GFP) and were commercially obtained from Cellworks. GFP-HUVEC were cultured in Endothelial Cell Growth Medium-2 consisting of Endothelial Cell Growth Basal Medium (EBM-2, Lonza #CC-3156 and CC-3162) and Endothelial Cell Growth Medium-2 Supplements (EGM-2, Lonza CC-4176) with 0.1 % GA-1000, 0.1 % R-IGF-1, 0.1 % VEGF, 0.1 % hEGF, 0.04 % hydrocortisone, 0.4 % hFGF-B, 0.1 % ascorbic acid, 0.1 % heparin). Instead of the fetal bovine serum supplied with the Kit, 2 % HS was used. The cells were expanded over 4 days and used between passages 4–5.

2.4. Cellular co-cultures for vascular network formation

The cells were harvested, split to aliquots, combined to yield 0.75 mio GFP-HUVEC and 0.15 mio hASC per sample (cell ratio 5:1) and centrifuged. The cell pellet was resuspended in NaGG, NaGG-avd, gelaCDH or gelaADH and placed into the well-plate (ibidi μ-slide 8-well, ibidi GmbH). The other component of each hydrogel was added and mixed swiftly using the pipette tip. The hydrogels were left to gelate at 37 °C for 30 min before adding 200 μL of EGM-2 on top. Media were changed three times a week. The samples were imaged live during the

culture period using EVOS microscope (EVOS FL Cell imaging system, Thermo Fisher Scientific) with brightfield view and GFP filter.

2.5. Immunofluorescent staining and image analysis

At day 14, co-culture samples were fixed using 4 % paraformaldehyde (PFA, Sigma, #158127) and unspecific binding was blocked with 10 % normal donkey serum (NDS, Sigma, #S30) in 1 % bovine serum albumin (BSA, Sigma, #A7906) solution containing 0.1 % TritonX-100 (Sigma, #T8787). All washing steps were performed using DPBS. The samples were consecutively treated with primary antibody (mouse monoclonal, α-smooth muscle actin, dilution 1:200, Abcam #ab7817) for 2 days, secondary antibody (Goat anti-Mouse IgG Alexa Fluor 568, dilution 1:400, Invitrogen # A-11004) overnight and finally DAPI (1:1000 in DPBS for 2 h). The GFP-HUVEC are visible due to their expressed GFP (GFP tagged HUVEC). The samples were imaged using confocal microscope Zeiss LSM 780 with 10× magnification objective and imaging approximately 200 μm per z-stack and EVOS images were clipped to remove the scale bar, and selected images were used for image analysis with AngioTool64 (Version 0.6a). The average vessel thickness was adjusted to around 10.4 ± 4.0 pixel units (confocal) and 4.2 ± 0.9 pixel units (EVOS). From the results, "vessels area" was used for further evaluation for endothelial cell coverage, which is the ratio of vessel area to explant ratio determined by the software.

2.6. Subcutaneous implantation

To study the materials *in vivo*, preformed samples were subcutaneously implanted to 40 male rats from the Wistar stock (60–90 days old), weighing 250–350 g. The species was selected in accordance the provisions of ISO10993-2. Experiments were carried out at the Unit of Comparative Biology at the Pontificia Universidad Javeriana (Bogota, Colombia), with the approval from the Institutional Committee for the Care and Use of Laboratory Animals (CICUAL-PUJ). The animals came from the internal colony of production which was initiated with a founding stock originating from Charles River, USA. There were 10 animals per time point, and each animal had 1 implant of each type (4 in total, $n = 10$). Before surgery, the animals were anesthetized using inhalation of 3 % isoflurane in oxygen flow set of 0.5 L/min. Rats under anesthesia were treated subcutaneously with meloxicam (1 mg/kg) and enrofloxacin (5 mg/kg) 30 min before the surgical incision. Hair was removed from the implant area and incisions were performed to create 4 pockets into the dorsal subcutaneous tissue by blunt dissection, so that the base of the pocket is at least 2 mm from the line of incision. Then, hydrogel implants (ø 10 mm and 1 mm in thickness) were inserted to the pocket. During the procedure, vital signs were monitored, and temperature support was placed. At the end of the procedure, the animals were allocated to the oxygenation chamber to recover from anesthesia. When the animals woke up showing good recovery, they were taken back to their cages. During the first three days after the procedure, the animals were medicated with meloxicam and enrifloxacin and the appearance of the incisions, signs of inflammation, infection or other events were evaluated. The animals were fed a standard diet and kept in groups of two in ventilated cages for the duration of the study. After 7, 14, 21 and 28 days of implantation, the animals were sacrificed using intraperitoneal sodium pentobarbital (50 mg/kg dose) and CO_2 inhalation. Each implant was collected separately, taking skin and subcutaneous tissues until reaching the fascia of the panniculus carnosa muscle and fixed in 10 % buffered formalin. The hydrogel degradation profile was followed during the retrieval.

2.7. Macroscopical and histological evaluation

Retrieved tissue samples were fixed with 10 % formalin, dehydrated in a series of alcohols, and embedded in paraffin. The paraffin-embedded specimens were sectioned to a thickness of 5 μm, and stained with hematoxylin and eosin (H&E). Stained sections were imaged with a Nikon Eclipse E 600 microscope and Toup Cam digital camera. Tissue lesions such as neutrophils, eosinophils, granulomatous reaction, giant cells and neovascularization were analyzed and semi-quantitatively scored on a scale from 0 to 3.

2.8. Statistical methods

Data from AngioTool evaluation were subjected to one-way ANOVA using Microsoft Excel Data Analysis ToolPak to test for significance. The results are displayed in Fig. 5. Normality of the data was assessed using chi-square test using a random data sample set with $n > 10$ from confocal image AngioTool analysis. With a p-value larger than 0.5 ($p = 0.97$), we assume the data to be normally distributed, and apply the same behavior also for data sets with low number of points that could not be tested.

3. Results

The scope of our work was to highlight and investigate the role of the material in cellular rearrangement and neovascularization. Firstly, we assessed the mechanical properties of the cell-free hydrogel materials. Though all materials investigated herein are based on GG (see Fig. 1), their crosslinking and viscoelastic behavior is drastically different. Rheological properties of the forming and formed hydrogels assessed by conducting time sweeps of the forming hydrogels and amplitude sweeps of fresh and degraded samples Similarly, their biochemical environment is different due to the addition of gelatin and fibronectin. Secondly, we observed the cell response of co-culture between hASC and HUVEC, which are well known to interact and form vascular networks, continuously monitored over 12 days, then fixed and stained on day 14. Finally, we investigated the *in vivo* tissue responses elicited by cell-free, preformed hydrogel samples after subcutaneous implantation in rats to observe acute tissue response within 4 weeks.

3.1. Rheological testing and degradation

In the pursuit to provide a thorough assessment and understanding of the viscoelastic properties, the materials were analyzed using rheology. A time sweep, with constant amplitude and frequency, gives the ability to observe time-dependent change of the hydrogel formation, *i.e.* the gelation. Gelation occurs as expected, as is shown in the previous publications [24,25,30]. Time point zero in Fig. 2A depicts few seconds after mixing of the two components, showing how long the hydrogel components take to form a solid network and suspend encapsulated cells. All materials form true hydrogels within the observation time of 1 h. While the gelation kinetics of NaGG and NaGG-avd, with final modulus of 552.8 ± 219.0 Pa and 493.2 ± 44.7 Pa respectively, are very similar, there is a stark difference between gelaCDH and gelaADH hydrogels. Though it could be expected these to be very similar judging from their chemical structure, gelaADH rapidly forms hydrogels with high modulus of 860.9 ± 6.6 Pa. GelaCDH has a delayed network formation and achieves a modulus of only 42.4 ± 7.7 Pa after 1 h.

In direct succession of the gelation sweep, after the sample was at rest for 5 min, an amplitude sweep was performed from 0.01 to 100 % oscillation strain as shown in Fig. 2B. The resting period ensures that the network is stress-free. Because storage (G′) is larger than loss modulus (G″) before the critical cross-over points, all materials are elastic solids. Before this crossover point of G′ and G″, where the moduli are constant, lies the linear viscoelastic region which indicates the elasticity of a hydrogel and reversible deformation. While a crossover point is observed for NaGG (48 % osc. strain) and NaGG-avd (32 % osc. strain) hydrogels, the observed range of oscillation strain is too short to reach irreversible deformation point for gelaCDH and gelaADH. The ratio between G″ and G′, *i.e.* tan δ, is proportional to the network density. A tan δ of 0.8 and 0.6 for NaGG and NaGG-avd, respectively, confirms the

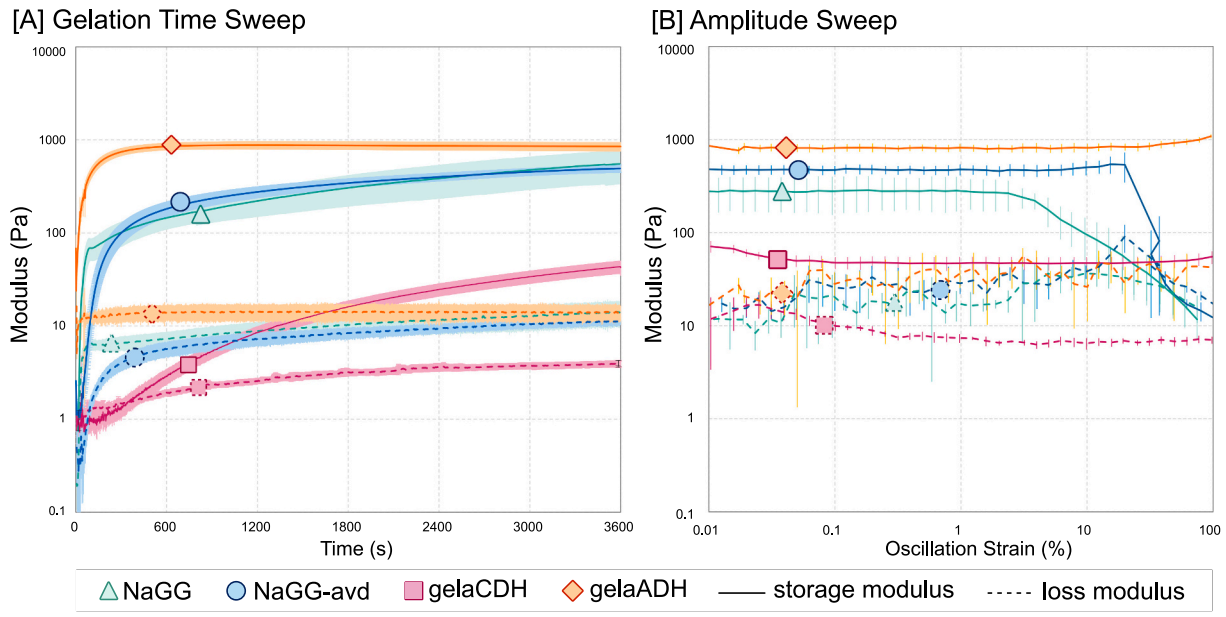

Fig. 2. Rheological assessment of cell-free hydrogels. (A) Time sweeps of hydrogels combined at $t = 7$ s. (B) Amplitude sweeps of samples just after gelation sweep. Solid line = storage modulus, dashed line = loss modulus.

finding of the time sweep that these two hydrogels are very similar and relatively tough. A comparison between the two gelatin-gels shows that CDH is softer (tan δ 0.16) and elastic than the very tough gelaADH gels presenting a very dense network (tan δ 0.04).

The flow behavior of the hydrogel precursors has been analyzed as well, showing again very similar flow behavior between NaGG and NaGG-avd precursors, while gelaADH dissolved in sucrose is slightly more viscous than gelaCDH dissolved in EBM-2. Surprisingly, the solvent has a great effect on GGox, resulting in higher viscosity and shear stress for sucrose solvent over cell culture medium, likely due to the effect of sugars on polysaccharides [33,34]. No direct comparison between precursor solution between the groups can be drawn here, as the respective solution concentrations are markedly different, with NaGG and NaGG-avd at 5 mg/mL, gelatin solutions at 40 mg/mL and oxidized GGox at 40 mg/mL. The data can be found in Appendix A1–1.

Cell-free samples were prepared similar to *in vivo* implantation procedure and incubated in EBM-2 at 37 °C for the specified time and their weight was observed, showing both swelling and mass loss due to degradation. NaGG and NaGG-avd hydrogels prove to be very stable, while gelatin-GG hydrogels quickly diminish in weight. This is also observed from the rheology analysis, where NaGG and NaGG-avd are stable and slightly increase their storage modulus, while the gelatin-based hydrogels quickly deteriorate. While measuring preformed samples with an amplitude sweep yields slightly different results compared to the method displayed in Fig. 2 and measuring highly degraded samples can have caveats. Nonetheless, when plotting the average value of the storage modulus at the linear viscoelastic region (LVER), shows expected behavior of sample types as seen in Fig. 3A. Both NaGG and NaGG-avd hydrogels show almost no degradation effects. Most noticeable is the increase in modulus, which is due to an increase in cross-linking by the medium and formation of more rigid network [33]. In contrast, the gelatin-GG hydrogels show rapid degradation. The modulus of gelaADH hydrogels declines rapidly and the measured samples were highly deformed. Unfortunately, it was not possible to measure the degradation products of gelaCDH at the other time points, and also the 6 h time point sample was delicate to measure.

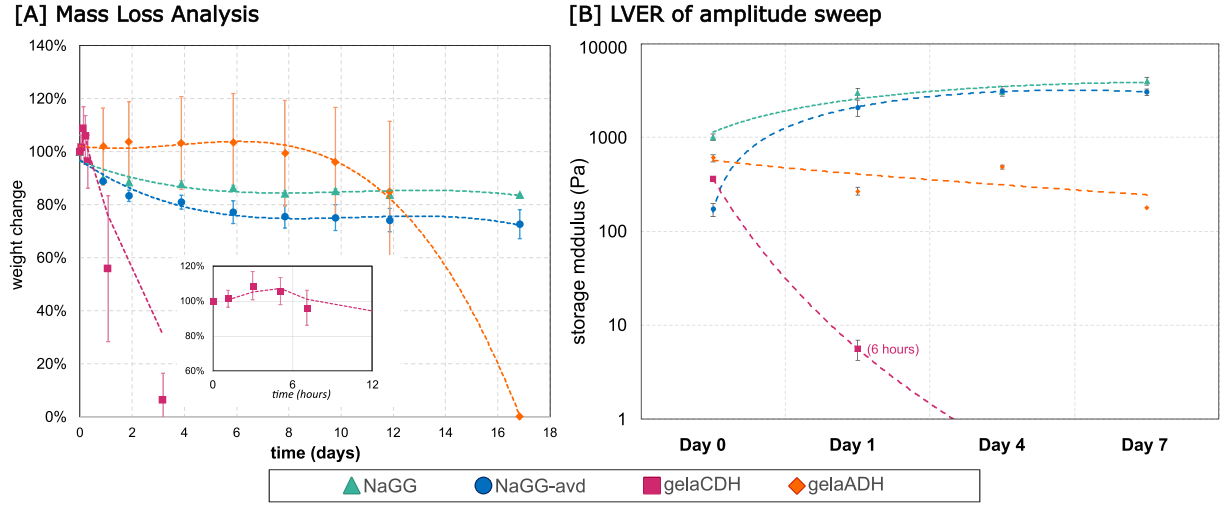

Fig. 3. Degradation of the investigated materials. [A] Mass loss analysis of cell-free materials in DMEM. Small inset image shows gelaCDH in degradation curve from 0 to 8 h. [B] Evolution of storage modulus at LVER in cell-free samples incubated in EBM-2 over 7 days.

Degradation of the hydrogels can also be observed from the EVOS images taken during the co-culture experiment. The low magnification (2×) captures the entire well and images are shown in Appendix A2–1. Upon close inspection a similar trend can be observed, where NaGG and NaGG-avd are highly stable, but a hole quickly forms in the center of gelaCDH and gelaADH samples. Hydrogel casting issues can lead to a premature degradation also for the NaGG and NaGG-avd hydrogels, but cell network formation appears to stabilize the hydrogel against degradation.

3.2. *In vitro co-culture results*

The encapsulation experiments show that HUVEC-hASC can be cultured in all four investigated materials up to 14 days, however with greatly varying results. Progression of the cell culture was monitored using EVOS microscope with brightfield and GFP filter on day 2, 4, 6, 9, and 12, example images of which can be viewed in Appendix A2–2. Already in the EVOS images, partial HUVEC elongation and network formation can be seen in the gelatin-gellan gum, but only sporadically for NaGG and NaGG-avd hydrogels (Appendix A2–2). Remarkably, also the progression of hydrogel degradation can be followed from 2× magnification in EVOS images (Appendix A2–1). Representative images of the confocal images at day 14 are shown in Fig. 4.

In the confocal images of NaGG and NaGG-avd the stained cells appear rounded and GFP-HUVEC are scattered and rounded. Modest elongation is visible in some of the NaGG-avd samples, but likely cells have migrated to the bottom of the well plate. The final molar concentrations of fibronectin protein modification in NaGG-avd were 71.0 nmol/L in the final hydrogel, compared to the avidin concentration of 1.6 μmol/L as determined in our previous publication [24]. The gelatin-containing samples (gelaCDH and gelaADH) on the other hand present a strong hASC network stained with αSMA. This network appears slightly denser in gelaCDH than gelaADH, but in both cases it is very pronounced. However, even in gelaCDH hydrogels the GFP-HUVEC do not form long, connected tubular structures, but alignment among the αSMA^{+} network can be observed in several locations.

AngioTool was used to measure the endothelial cell (EC) coverage from the EVOS images (Fig. 5A), as well as the αSMA^{+} cell coverage of the confocal images (Fig. 5B). Because presence of interconnected tubule network was not observed, the total coverage of ECs and αSMA cells was considered. NaGG shows a fast loss of EC coverage between day 2 and 4, and no recovery, while NaGG-avd presents an initial increase in EC coverage from day 2 to 4, followed by a steady decline. The gelaCDH hydrogels produce a small initial dip in EC coverage, but an increase from day 6 onward is visible. Finally, gelaADH shows an initial decline, but between day 4 and day 12 there are no significant differences ($p < 0.5$).

The cell coverage assessment of the αSMA^{+} network from the confocal images confirms the visual observations. While gelaCDH presents a dense network (27.6 % coverage), and gelaADH is near similar in strength (17.4 % coverage), the total coverage for NaGG and NaGG-avd hydrogels is significantly lower (12.0 % and 5.4 %). Due to degradation issues, only few samples of NaGG-avd could be assessed, likely leading to skewed values towards the lower end. Remarkably, the plots of EVOS

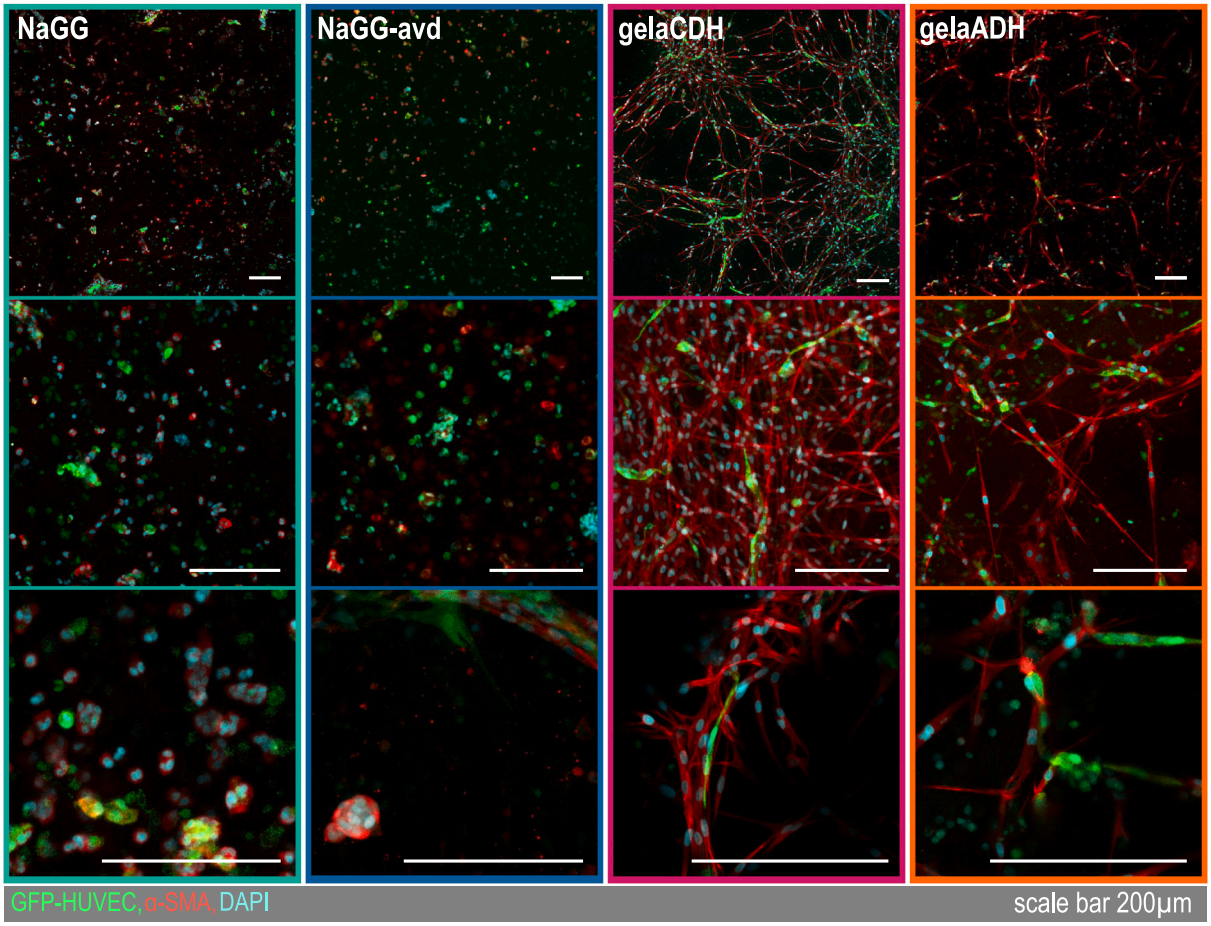

Fig. 4. Confocal microscope images of *in vitro* co-culture samples at day 14 after encapsulation. Red = αSMA, green = GFP-HUVEC, blue = DAPI cell nuclei, scale bar is 200 μm. All images were taken with 10× objective, top row shows a tile stack (1790 × 1790 μm), center row standard stack (639 × 639 μm), and bottom row small stack (310 × 310 μm).

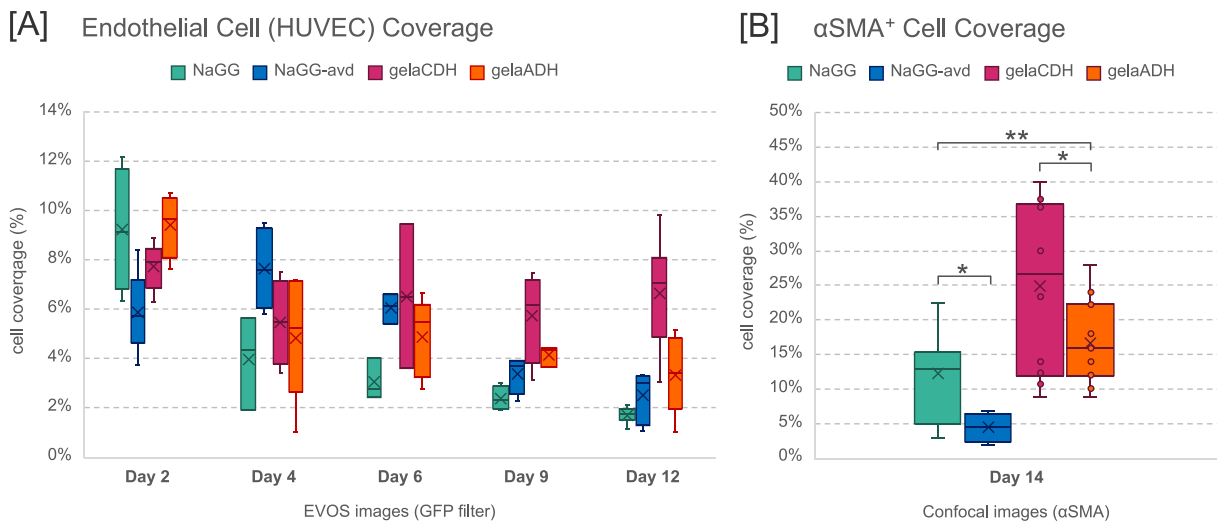

Fig. 5. Percentage of images covered with (A) endothelial and (B) αSMA positive cells, representing network formation. (A) GFP-HUVEC channel/signal from 4× magnification images on day 2, 4, 6, 9 and 12. (B) αSMA signal from confocal microscope images (pooled) at day 14. Images were analyzed using AngioTool.

day 12 and confocal day 14 seem to resemble each other in distribution between the investigated materials.

3.3. Macroscopic and histologic evaluation of the hydrogel implants

The animals tolerated the implantation procedure well and did not show adverse reaction (Appendix A4). All the animals behaved normally throughout the observation period after the implant surgery and scabbing was absent or lightweight. None of the animals developed severe oedema, and signs of oedema were entirely absent towards final time points. The hydrogel implants decrease in size between 70 and 50 % during the 28 days evaluation period. Some of the implants moved in the subcutaneous area during the evaluation period. The microscopical evaluation indicated that the implants did not affect the epidermis, dermis or adipic panniculus. The subcutaneous tissue showed diffuse lesions not related with the implant but with the surgical procedure, like oedema, infiltration of mononuclear cells and mast cells. Macroscopic assessment of the retrieved samples and their presence is tabulated in Appendix A3.

The findings from the tissue scoring associated with the implant are summarized in Table 2, where cell presence was rated on a scale from 0 to 3. Tissue slices for day 28 and examples of evaluated features are shown in Fig. 6. A more complete selection of histology images can be found in Appendix A5. In general, foreign body reaction was found to be more pronounced in the bioactivated formulations (NaGG-avd, gelaCDH, gelaADH), and even more so in the gelatin-containing formulations (gelaCDH, gelaADH).

Most prominently, neovascularization around the implant is much more pronounced in both gelatin-composite hydrogels. While gelaCDH shows steady signs of neovascular vessels throughout day 7 to 28, gelaADH has a muted response until day 28, where it achieves the highest score observed within these samples. Neovascularization is slightly more effective in NaGG-avd over pure NaGG, owing to the added fibronectin. There is no direct ingrowth of blood vessels observed into any of the implants. NaGG is the only material without lymphocytic infiltrate, while the other, bioactivated materials induce stronger reactions. Granulomatous reaction and giant cell presence are also greatly increased in the bioactivated hydrogels, especially for the gelatin-containing formulations. A mild capsule formation, indicated also by the presence of multinucleated giant cells, is observed for all implants.

Only the NaGG hydrogels at time points over 14 days showed no granulomatous reaction, all the other samples and time points had evidence of mild to moderate reaction. The gelaADH hydrogel samples showed severe granulomatous reaction at later time points. The presence of giant cells follows similar observations as granuloma, where all samples have mild to moderate giant cell presence. Only NaGG hydrogels show no evidence of giant cells at final time points, while gelaADH hydrogels induce a severe reaction at day 14. No lymphoplasmacytic (LP) infiltrate was observed for NaGG hydrogels on any evaluated time points, while the bioactivated hydrogels showed mild LP infiltrate at earlier time points, and moderate infiltrate towards 28 days.

4. Discussion

Cellular responses *in vitro* and *in vivo* are controlled by a complex combination of surrounding microenvironmental factors including biochemical cues and mechanical support. Native GG is known to be cyto- and biocompatible, albeit not bioactive and cells do not attach to

Table 2
Scoring results of subcutaneous implants. Biopsy slices were fixed in paraffin, stained with hematoxylin and eosin and scored with a scale from 0 to 3 and visualized with + and −.

	NaGG				NaGG-avd				gelaCDH				gelaADH			
Day	7	14	21	28	7	14	21	28	7	14	21	28	7	14	21	28
Neovascularization	+	−	−	−	+	+	−	+	++	+	++	++	+	+	+	+++
Diffuse mast cells	+	+	−	−	+	+	−	−	+	+	++	++	+	+	+	++
Granulomatous reaction	+	+	−	−	+	++	+	+	++	+++	++	++	++	+++	+	+++
Giant cell presence	+	+	−	−	+	++	+	+	++	++	++	++	++	+++	+	++
Neutrophils	−	−	−	−	−	−	−	−	−	−	+	−	−	−	−	−
Eosinophils	−	−	−	−	+	−	−	−	+	−	−	+	+	−	−	+
Lymphocytic infiltrate	−	−	−	−	+	++	+	+	+	++	++	++	+	++	+	++
# of retrieved samples	6	7	4	7	9	9	7	7	10	8	4	4	7	10	3	2

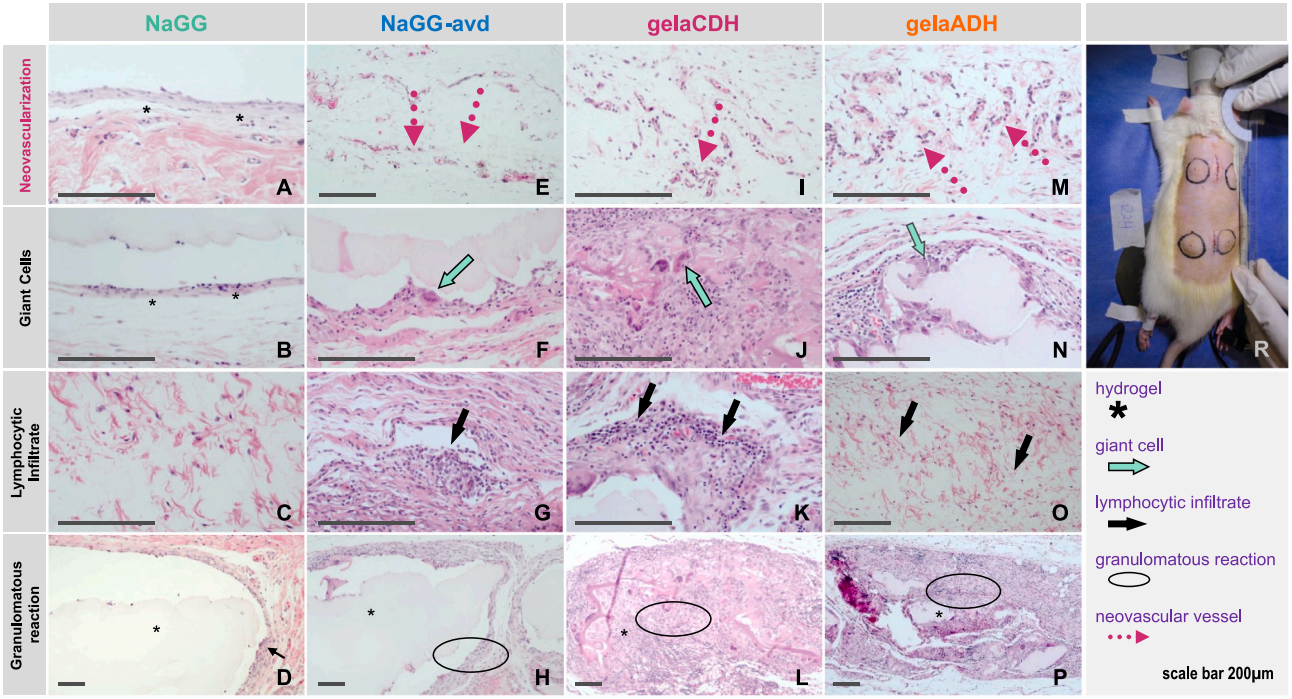

Fig. 6. Exemplary histology slices showing relevant features on day 28. Asterisk (*) indicates the implanted hydrogel. Markers show the following features: Neovascular vessel (A, E, I, M), Giant cell infiltration (B none|F mild|J, N moderate), Lymphocytic infiltrate (C none|G, O mild|K moderate), and Granulomatous reaction (D none|H mild|L moderate|P severe); Hydrogels types are A–D NaGG, E–H NaGG-avd, I–L gelaCDH, M–P gelaADH. Image R shows an example of the implantation sites immediately after surgery.

its polymer structure. To make use of its excellent mechanical properties and availability, many bioactivation strategies have been proposed [15,35–37]. Here, we aimed to investigate bioactivation strategies previously described by our lab in more detail, while directly comparing the three aspects of mechanical properties, *in vitro* cell response and *in vivo* tissue activity, in order to highlight the relation of these features. The hydrogel polymers are formulated in cell culture media, HEPES buffer or sucrose (10 %), which ensures an appropriate osmotic concentration for cell survival. After gelation, cell culture medium was added on top of the hydrogels, which readily diffuses through the hydrogels [38]. During the cell culture experiment, ionic strength and pH are both regulated by addition of cell culture medium on top, and thus they are similar for all investigated materials.

The structural analysis of the investigated materials has been reported extensively in previous publications. Ion concentration of the purified NaGG and functionalized NaGG-avd were determined using ICP-OES, with $Ca^{2+} < 0.1$ wt% and $Na^{+} \geq 2.5$ wt% [24]. The presence of ADH and CDH functional groups in modified gelatin have been confirmed by ^{1}H NMR results [25]. The oxidation degree of GGox has been determined *via* aldehyde UV titration, which showed that over 25 % of available rhamnose rests in the GG repeat unit have been oxidized [30]. Using fluorescence titration, the avidin modification degree of NaGG-avd has been determined to reach up to 0.375 µmol per mg NaGG-avd [24]. All hydrogel formulations have previously been subjected to uniaxial, unconfined compression at a rate of 10 mm/min. The recorded fracture strength of the gelatin-gellan gum formulations is much higher with 20.4 ± 1.8 kPa and 61.6 ± 14.1 kPa for gelaADH and gelaCDH (1:1 formulations with GGox) [25] as compared to the very brittle NaGG-Ca and NaGG-avd-SPD with 5.1 ± 0.8 kPa and 6.4 ± 1.2 kPa respectively. Similarly, the fracture strain is shifted to higher values for gelaCDH (69.9 ± 2.9 %) and gelaADH (61.7 ± 5.0 %) when compared to NaGG (45.5 ± 1.0 %) and NaGG-avd (36.5 ± 5.6 %), underlining the more elastic nature of the gelatin-gellan gum hydrogels.

The hydrogel formulations were analyzed using rheological amplitude and time sweep, taking advantage of the ability to investigate the viscoelastic properties of the as-prepared hydrogels. The rheological time sweep shows that NaGG and NaGG-avd hydrogels are very stiff, but they form gels reliably and fast. The gelaCDH hydrogels are softer and form slowly, while gelaADH presents a high modulus and forms hydrogels very quickly. The extent of the LVER in the amplitude sweep shows that gelatin-GG hydrogel formulations are much more elastic than NaGG-based hydrogels. Viscoelastic properties have been acknowledged to greatly affect cell response and a cell's ability to interact with the material *via* mechanotransduction [1,10,39]. However, material design is an interplay of density, stiffness, viscoelasticity, and degradation, as well presentation and concentration of bioactive and cell attachments motifs [5]. While it was reported that HUVEC have increased expression of VEGF in substrates with lower stiffness [39], angiogenic sprouting has been shown to favor stiffer matrices [40]. As confirmed in our amplitude sweep, pure NaGG hydrogels are rather brittle materials, which is often observed for ionically crosslinked hydrogels [33]. All formulations investigated here form hydrogels fast enough to effectively encapsulate cells for true 3D cell culture, but with sufficient delay to permit casting them to the well plate or into a mold. In regard to the previously assessed compressive behavior, Koivisto et al. (2019) showed that gelaCDH and gelaADH-based hydrogels have a very similar fracture strain and strength, very elastic and brittle [25], although gelaCDH is more elastic. Also NaGG and NaGG-avd have been compared using compression testing and have very similar fracture and strain behavior [24]. When comparing the mechanical properties of our presented hydrogels, their composition and total polymer concentration must be taken into account. NaGG and NaGG-avd are formulated at 8-fold lower concentration than the gelatin-containing samples yet prove to be similar in modulus with lower elasticity. Bioactivity appears to be governed through the addition of gelatin, as well as elasticity and compliance.

Preformed samples could also be analyzed for degradation testing, although measuring highly degraded samples is rather challenging. The performed test does not directly imitate neither *in vitro* nor *in vivo* experiments due to omission of cells, however, a general trend of biomaterial degradation development can be gauged. NaGG and NaGG-avd

have been found to be very stable, but this strongly depends on the success of mixing with the crosslinker, as well as the casting step. Issues were observed in the cell culture experiment with stability of NaGG and NaGG-avd formulations, but that may have been due to inadequate mixing. On the other hand, gelaCDH degrades rapidly *in vitro* without cells, even without serum in the supernatant. In turn, this hydrogel formulation was surprisingly stable in the cell culture experiments, likely due to ECM production of cells stabilizing the construct. Finally, gelaADH hydrogels are more stable, but during the rheology experiments the samples changed appearance and mechanical properties more strongly than NaGG and NaGG-avd hydrogel. Conversely, Koivisto et al. (2019) investigated the degradation of gelaCDH and gelaADH formulations using collagenase and found that ADH degrades more swiftly compared to CDH, which was concluded to be due to higher crosslinking density [25].

The co-culture of HUVEC and hASC or similar mesenchymal stem cells (hMSC) has been shown to promote vasculogenesis and self-assemble to form vascular network with and without additional biomaterial support [17,19,41]. Andree et al. (2019) showed that in serum-free conditions hASC and HUVEC are forming functional vessels in different collagen matrices, however their study provides no assessment of mechanical properties for the used materials. Interestingly, the authors conclude that this co-culture system could be used for supporting rearrangement of target cell types in *e.g.* the formation of smooth muscle cell network, which is strongly reflected by our findings [17]. Similarly, Kim et al. (2022) developed bioprinted collagen-β-TCP scaffolds and showed the co-culture of hASC and HUVEC specifically for osteogenesis and vasculogenesis [41].

Vasculogenesis is indicated by the elongation and network formation of EC, and development of an interconnected network from these. From the confocal images, we detected a formation of endothelial cell clusters and aggregates and short tubule structures but no interconnected vascular network in any hydrogel formation. However, gelatin-containing formulations included significantly more extensive endothelial cell coverage compared to NaGG-based hydrogel formulations. A more pronounced cell network was visible in NaGG-avd on day 12 (Appendix A2–2), but these samples did not endure the staining procedure and were not possible to image using confocal microscopy Overall, NaGG and NaGG-avd seemingly prevent cell network formation, but nonetheless are cytocompatible materials supporting their viability. The effective addition of biotinylated compounds to NaGG-avd at 1.5 μM per 1 mL hydrogel has been shown previously [24], but also in our originally study we concluded this concentration to be too low to achieve noticeable cell response. Surprisingly, despite the incapability to support vascular network formation, gelatin-based formulations rapidly produced an extensive αSMA-positive cellular network. The co-localization of HUVEC and αSMA-positive cells suggests close interaction of the two cell types as detected in our earlier vessel formation studies [23].

While gelaCDH and gelaADH hydrogel formulations are similar in chemical structure and in availability of gelatin, which provides cell interaction, the cell response does show significant differences in endothelial cell coverage. This is likely due to considerable difference in viscoelastic response as observed from the rheological amplitude sweeps. GelaCDH hydrogels are more elastic, while gelaADH hydrogels are quite rigid and have a higher modulus. While it has been reported that angiogenic sprouting is more pronounced in stiffer substrates [40,42], this is not observed when comparing gelaCDH and gelaADH here. However, it is also known that cells prefer a permissive matrix, which improves ability to remodel and deposit own ECM [43], seemingly favoring our gelaCDH formulation.

The results from the animal study are overall in line with the cell culture results: Hydrogels from NaGG are rather inert, NaGG-avd and its fibronectin modification shows a slight upward trend in tissue response, while a strong response is observed from both gelatin-GG formulations, as indicated by the inflammatory markers and neovascular vessel growth around the implants. There was no vascular ingrowth into any of the studied hydrogels, however the implants were cell-free and such auto-vascularization would not be expected. Interestingly, Desai et al. (2015) observed cell infiltration to cell-free hydrogel when observing their injectable, RGD-modified alginate norbornene-click hydrogels [44]. This effect was likely due to physical fragmentation of their ionically crosslinked formulations, which also have been described to be less stable than the covalent photo-crosslinked formulation. Similarly, compared to our crosslinked hydrogel formulations most injectable hydrogels in the literature are much softer, which more easily allow for cell infiltration and remodeling [45,46].

The presence of macrophages in the early time points indicates a positive, acute immune response, while their absence in later time points suggests no chronic inflammation. Similar to our study, Silva-Correia et al. (2013) reported the subcutaneous implantation of cell-free methacrylated GG (GG-MA) photo-crosslinked disks into rats [26]. In line with the expectation that GG-MA is as bioinert as native GG, they observed a moderate infiltration of granulocytes and macrophages into their hydrogels, and complete clearance of immune response markers 3 weeks of implantation.

The chosen implantation time of 28 days is too short to fully assess a mature tissue response and incorporation, but the initial implantation response and acute inflammation can be surveyed. All implanted hydrogels showed foreign body reaction to different degrees and a mild fibrosis. Absence of neutrophils indicates a successful and clean implantation procedure and no adverse inflammation reaction. Similarly, the low count of eosinophils indicates that the materials did not cause any allergic reaction. It is understood that the source of gelatin plays a significant role in immune response [47,48]. We have compared standard cell culture grade gelatin and ultra-low endotoxin gelatin in a preliminary cell culture experiment. The gelatins showed no difference in cell proliferation and morphology (Appendix 6). However, this test might not be directly translatable to *in vivo* tissue reaction. Relevant foreign body reaction was observed during tissue implantation for gelatin-containing hydrogels.

In summary, our observations show that in order to steer cell response *via* mechanotransduction, biomaterial design requires adequate mechanical properties, as defined by viscoelasticity and stiffness, as well as cell attachment, in order to convey the mechanical properties to the cell. Hence, the bioactivation strategy of GG covalently coupling functionalized gelatin (gelaCDH and gelaADH) succeeds in supporting an extensive cellular network and elicits neovascular response *in vivo* than the bioinert NaGG. The addition of fibronectin *via* avidin-biotin coupling in NaGG-avd shows a similar, albeit muted, tendency, likely due to low modification rate [24]. While this work did not aim for a decoupling of viscoelasticity and presentation of bioactive factors within the range of tested biomaterials, we present a comparative insight to vascular network formation *in vitro* and tissue response including neovascularization *in vivo*.

5. Conclusions

We have investigated the chemical modification of the bacterial polysaccharide GG, in an effort to render it more bioactive towards vascularization *in vitro* and *in vivo*. All hydrogels were tested for their rheological properties and gelation time frame, showing that NaGG and NaGG-avd are less elastic than either of the gelatin formulations, and that gelaADH is magnitudes more rigid than gelaCDH. A co-culture of HUVEC and hASC was encapsulated in each hydrogel formulation, as this combination of cell types self-assembles to vascular network. None of our investigated hydrogels formed strong endothelial networks, despite cell attachment sites being provided *via* gelatin. Instead, the gelatin-containing hydrogel strongly supported hASC proliferation and formation of αSMA^{+} cellular network. Biocompatibility of the hydrogels was surveyed by subcutaneous implantation into a rat model for up to 4 weeks. The muted immune response of NaGG and NaGG-avd-b-

fibronectin can be advantageous for inert implantation applications, while the stronger immune response of the gelatin-gellan gum hydrogels proves their general bioactivity. All materials were found to be biocompatible, and no adverse inflammation or host response was observed, but early signs of neovascularization were observed. In summary, we have presented versatile bioactivation strategies for gellan gum, as well as a thorough *in vitro* and *in vivo* testing. Our findings indicate a strong relation between biomechanical properties of a hydrogel and biological responses.

CRediT authorship contribution statement

Christine Gering: Conceptualization, Methodology, Formal analysis, Investigation, Data Curation, Writing, Review & Editing, Visualization; **Jenny Parraga**: Conceptualization, Investigation, Writing, Review & Editing; **Hanna Vuorenpää**: Conceptualization, Validation, Investigation, Writing, Review & Editing; **Lucía Botero**: Methodology, Formal analysis, Resources, Data Curation, Writing; **Susanna Miettinen**: Conceptualization, Validation, Resources, Review & Editing, Supervision, Funding acquisition; **Minna Kellomäki**: Conceptualization, Resources, Review & Editing, Supervision, Funding acquisition.

Declaration of competing interest

The authors declare that they have no known competing financial interests or personal relationships that could have appeared to influence the work reported in this paper.

Data availability

The original contributions presented in the study are included in the article and in the Supplementary materials, further inquiries can be directed to the corresponding author.

Acknowledgements

This work was financially supported by the Academy of Finland through the CoEBoC projects of Minna Kellomäki (312409 and 326587, 336663), and Susanna Miettinen (336666, 326588, 312413). We wish to thank Kirsi Penttinen for carrying out the gelatin coating test, as well as Anna-Maija Honkala and Sari Kalliokoski for their excellent technical assistance. We are further grateful to the Tampere Imaging facilities for assistance with confocal microscopy and image analysis.

Appendix A. Supplementary data

Supplementary data to this article can be found online at https://doi.org/10.1016/j.bioadv.2022.213185.

References

[1] J. Rouwkema, A. Khademhosseini, Vascularization and angiogenesis in tissue engineering: beyond creating static networks, Trends Biotechnol. 34 (9) (2016) 733–745, https://doi.org/10.1016/j.tibtech.2016.03.002.
[2] C. McKee, G.R. Chaudhry, Advances and challenges in stem cell culture, Colloids Surf. B: Biointerfaces 159 (2017) 62–77, https://doi.org/10.1016/j.colsurfb.2017.07.051.
[3] R. Chapla, J.L. West, Hydrogel biomaterials to support and guide vascularization, Prog. Biomed. Eng. 3 (1) (2021), 012002, https://doi.org/10.1088/2516-1091/abc947.
[4] R. Lanza, R. Langer, J.P. Vacanti, Principles of Tissue Engineering, Fourth edi., Academic Press, US, 2014.
[5] C.O. Crosby, J. Zoldan, Mimicking the physical cues of the ECM in angiogenic biomaterials, Regen. Biomater. 6 (2) (2019) 61–73, https://doi.org/10.1093/rb/rbz003.
[6] R. Kocen, M. Gasik, A. Gantar, S. Novak, Viscoelastic behaviour of hydrogel-based composites for tissue engineering under mechanical load, Biomed. Mater. (Bristol, U. K.) 12 (2) (2017) 25004, https://doi.org/10.1088/1748-605x/aa5b00.
[7] F. Lee, M. Kurisawa, Formation and stability of interpenetrating polymer network hydrogels consisting of fibrin and hyaluronic acid for tissue engineering, Acta Biomater. 9 (2) (Feb. 2013) 5143–5152, https://doi.org/10.1016/J.ACTBIO.2012.08.036.
[8] R. Yao, R. Zhang, F. Lin, J. Luan, Biomimetic injectable HUVEC-adipocytes/collagen/alginate microsphere co-cultures for adipose tissue engineering, Biotechnol. Bioeng. 110 (5) (2013) 1430–1443, https://doi.org/10.1002/bit.24784.
[9] M.B. Oliveira, C.A. Custódio, L. Gasperini, R.L. Reis, J.F. Mano, Autonomous osteogenic differentiation of hASCs encapsulated in methacrylated gellan-gum hydrogels, Acta Biomater. 41 (2016) 119–132, https://doi.org/10.1016/j.actbio.2016.05.033.
[10] A.J. Engler, S. Sen, H.L. Sweeney, D.E. Discher, Matrix elasticity directs stem cell lineage specification, Cell 126 (4) (Aug. 2006) 677–689, https://doi.org/10.1016/j.cell.2006.06.044.
[11] T. Muthukumar, J.E. Song, G. Khang, Biological role of gellan gum in improving scaffold drug delivery, cell adhesion properties for tissue engineering applications, Molecules (Basel, Switzerland) 24 (24) (2019) 4514, https://doi.org/10.3390/molecules24244514.
[12] M. Das, T.K. Giri, Hydrogels based on gellan gum in cell delivery and drug delivery, J. Drug Delivery Sci. Technol. 56 (Apr. 2020), 101586, https://doi.org/10.1016/J.JDDST.2020.101586.
[13] P. Matricardi, C. Cencetti, R. Ria, F. Alhaique, T. Coviello, Preparation and characterization of novel gellan gum hydrogels suitable for modified drug release, Molecules 14 (9) (2009) 3376–3391, https://doi.org/10.3390/molecules14093376.
[14] Y. Gong, C. Wang, R.C. Lai, K. Su, F. Zhang, D. Wang, An improved injectable polysaccharide hydrogel: modified gellan gum for long-term cartilage regenerationin vitro, J. Mater. Chem. 19 (14) (2009) 1968–1977, https://doi.org/10.1039/B818090C.
[15] L.A. Rocha, et al., In vitro evaluation of ASCs and HUVECs co-cultures in 3D biodegradable hydrogels on neurite outgrowth and vascular organization, Front. Cell Dev. Biol. 8 (June) (2020) 1–14, https://doi.org/10.3389/fcell.2020.00489.
[16] N.A. Silva, et al., The effects of peptide modified gellan gum and olfactory ensheathing glia cells on neural stem/progenitor cell fate, Biomaterials 33 (27) (2012) 6345–6354, https://doi.org/10.1016/j.biomaterials.2012.05.050.
[17] B. Andrée, et al., Formation of three-dimensional tubular endothelial cell networks under defined serum-free cell culture conditions in human collagen hydrogels, Sci. Rep. 9 (1) (2019) 1–11, https://doi.org/10.1038/s41598-019-41985-6.
[18] M. Ermis, Photo-crosslinked gelatin methacrylate hydrogels with mesenchymal stem cell and endothelial cell spheroids as soft tissue substitutes, J. Mater. Res. 36 (1) (2021) 176–190, https://doi.org/10.1557/s43578-020-00091-4.
[19] J.-R. Sarkanen, et al., Adipose stromal cell tubule network model provides a versatile tool for vascular research and tissue engineering, Cells Tissues Organs 196 (5) (Oct. 2012) 385–397, https://doi.org/10.1159/000336679.
[20] J. Liu, Y.J. Chuah, J. Fu, W. Zhu, D.A. Wang, Co-culture of human umbilical vein endothelial cells and human bone marrow stromal cells into a micro-cavitary gelatin-methacrylate hydrogel system to enhance angiogenesis, Mater. Sci. Eng. C 102 (Sep. 2019) 906–916, https://doi.org/10.1016/J.MSEC.2019.04.089.
[21] U. Blache, S. Metzger, Q. Vallmajo-Martin, I. Martin, V. Djonov, M. Ehrbar, Dual role of mesenchymal stem cells allows for microvascularized bone tissue-like environments in PEG hydrogels, Adv. Healthc. Mater. 5 (4) (2016) 489–498, https://doi.org/10.1002/adhm.201500795.
[22] S. Hauser, F. Jung, J. Pietzsch, Human endothelial cell models in biomaterial research, Trends Biotechnol. 35 (3) (Mar. 2017) 265–277, https://doi.org/10.1016/J.TIBTECH.2016.09.007.
[23] A. Mykuliak, et al., Vasculogenic potency of bone marrow- and adipose tissue-derived mesenchymal stem/stromal cells results in differing vascular network phenotypes in a microfluidic Chip, Front. Bioeng. Biotechnol. (Feb. 2022) 60, https://doi.org/10.3389/FBIOE.2022.764237.
[24] C. Gering, et al., Design of modular gellan gum hydrogel functionalized with avidin and biotinylated adhesive ligands for cell culture applications, PLoS ONE 14 (8) (Aug. 2019) 1–22, https://doi.org/10.1371/journal.pone.0221931.
[25] J.T. Koivisto, et al., Mechanically biomimetic gelatin-gellan gum hydrogels for 3D culture of beating human cardiomyocytes, ACS Appl. Mater. Interfaces 11 (23) (2019) 20589–20602, https://doi.org/10.1021/acsami.8b22343.
[26] J. Silva-Correia, et al., Biocompatibility evaluation of ionic- and photo-crosslinked methacrylated gellan gum hydrogels. In vitro and in vivo study, Adv. Healthc. Mater. 2 (4) (2013) 568–575, https://doi.org/10.1002/adhm.201200256.
[27] L.R. Stevens, J. Gilmore, G.G. Wallace, G.G.M. in het Panhuis, Tissue engineering with gellan gum, Biomater. Sci 4 (9) (2016) 1276–1290, https://doi.org/10.1039/c6bm00322b.
[28] C.J. Ferris, et al., Peptide modification of purified gellan gum, J. Mater. Chem. B 3 (6) (2015) 1106–1115, https://doi.org/10.1039/c4tb01727g.
[29] V.P. Hytönen, et al., Design and construction of highly stable, protease-resistant chimeric avidins, J. Biol. Chem. 280 (11) (2005) 10228–10233, https://doi.org/10.1074/jbc.M414196200.
[30] C. Gering, A. Rasheed, J.T. Koivisto, J. Párraga, S. Tuukkanen, M. Kellomäki, Chemical modification strategies for viscosity-dependent processing of gellan gum, Carbohydr. Polym. 269 (2021), 118335, https://doi.org/10.1016/j.carbpol.2021.118335.
[31] L. Kyllönen, et al., Effects of different serum conditions on osteogenic differentiation of human adipose stem cells in vitro, Stem Cell Res Ther 4 (1) (2013) 17, https://doi.org/10.1186/scrt165.
[32] M. Dominici, et al., Minimal criteria for defining multipotent mesenchymal stromal cells. The International Society for Cellular Therapy position statement, Cytotherapy 8 (4) (Jan. 2006) 315–317, https://doi.org/10.1080/14653240600855905.

[33] E.R. Morris, K. Nishinari, M. Rinaudo, Gelation of gellan - a review, Food Hydrocoll. 28 (2) (Aug. 2012) 373–411, https://doi.org/10.1016/j.foodhyd.2012.01.004.
[34] V. Evageliou, M. Mazioti, I. Mandala, M. Komaitis, Compression of gellan gels. Part II: effect of sugars, Food Hydrocoll. 24 (4) (2010) 392–397, https://doi.org/10.1016/j.foodhyd.2009.11.005.
[35] L.P. da Silva, A.K. Jha, V.M. Correlo, A.P. Marques, R.L. Reis, K.E. Healy, Gellan gum hydrogels with enzyme-sensitive biodegradation and endothelial cell biorecognition sites, Adv. Healthc. Mater. 7 (5) (2018) 1–12, https://doi.org/10.1002/adhm.201700686.
[36] E.D. Gomes, et al., Combination of a peptide-modified gellan gum hydrogel with cell therapy in a lumbar spinal cord injury animal model, Biomaterials 105 (Supplement C) (2016) 38–51, https://doi.org/10.1016/j.biomaterials.2016.07.019.
[37] C.A. Vilela, et al., In vitro and in vivo performance of methacrylated gellan gum hydrogel formulations for cartilage repair*, J. Biomed. Mater. Res. A 106 (7) (2018) 1987–1996, https://doi.org/10.1002/jbm.a.36406.
[38] A.M. Soto, et al., Optical projection tomography technique for image texture and mass transport studies in hydrogels based on gellan gum, Langmuir 32 (20) (2016) 5173.
[39] L. Santos, et al., Extracellular stiffness modulates the expression of functional proteins and growth factors in endothelial cells, Adv. Healthc. Mater. 4 (14) (2015) 2056–2063, https://doi.org/10.1002/adhm.201500338.
[40] B.N. Mason, A. Starchenko, R.M. Williams, L.J. Bonassar, C.A. Reinhart-King, Tuning three-dimensional collagen matrix stiffness independently of collagen concentration modulates endothelial cell behavior, Acta Biomater. 9 (1) (Jan. 2013) 4635–4644, https://doi.org/10.1016/J.ACTBIO.2012.08.007.
[41] W.J. Kim, H. Lee, E. Ji Roh, S. Bae An, I.B. Han, G. Hyung Kim, A multicellular bioprinted cell construct for vascularized bone tissue regeneration, Chem. Eng. J. 431 (Mar. 2022), 133882, https://doi.org/10.1016/J.CEJ.2021.133882.
[42] J. He, Y. Du, J.L. Villa-Uribe, C. Hwang, D. Li, A. Khademhosseini, Rapid generation of biologically relevant hydrogels containing long-range chemical gradients, Adv. Funct. Mater. 20 (1) (Jan. 2010) 131–137, https://doi.org/10.1002/ADFM.200901311.
[43] M.W. Tibbitt, K.S. Anseth, Hydrogels as extracellular matrix mimics for 3D cell culture, Biotechnol. Bioeng. 103 (4) (2009) 655–663, https://doi.org/10.1002/bit.22361.
[44] R.M. Desai, S.T. Koshy, S.A. Hilderbrand, D.J. Mooney, N.S. Joshi, Versatile click alginate hydrogels crosslinked via tetrazine–norbornene chemistry, Biomaterials 50 (2015) 30–37, https://doi.org/10.1016/j.biomaterials.2015.01.048.
[45] N.A. Silva, et al., The effects of peptide modified gellan gum and olfactory ensheathing glia cells on neural stem/progenitor cell fate, Biomaterials 33 (27) (Sep. 2012) 6345–6354, https://doi.org/10.1016/j.biomaterials.2012.05.050.
[46] I. Noshadi, et al., In vitro and in vivo analysis of visible light crosslinkable gelatin methacryloyl (GelMA) hydrogels, Biomater. Sci. 5 (10) (Sep. 2017) 2093–2105, https://doi.org/10.1039/C7BM00110J.
[47] A.B. Bello, D. Kim, D. Kim, H. Park, S.H. Lee, Engineering and functionalization of gelatin biomaterials: from cell culture to medical applications, Tissue Eng. B Rev. 26 (2) (Apr. 2020) 164–180, https://doi.org/10.1089/TEN.TEB.2019.0256.
[48] A. Magnusdottir, H. Vidarsson, J.M. Björnsson, B.L. Örvar, Barley grains for the production of endotoxin-free growth factors, Trends Biotechnol. 31 (10) (Oct. 2013) 572–580, https://doi.org/10.1016/J.TIBTECH.2013.06.002.